This information is current as of October 11, 2024.

Patterns of Intrathecal Ossification in Arachnoiditis Ossificans: A Retrospective Case Series

B. Thejeel, C.S. Geannette, M. Roytman, D.J. Pisapia, J.L. Chazen and S.T. Jawetz

AJNR Am J Neuroradiol 2023, 44 (2) 228-234
doi: https://doi.org/10.3174/ajnr.A7764
http://www.ajnr.org/content/44/2/228

Patterns of Intrathecal Ossification in Arachnoiditis Ossificans: A Retrospective Case Series

B. Thejeel, C.S. Geannette, M. Roytman, D.J. Pisapia, J.L. Chazen, and S.T. Jawetz

ABSTRACT

SUMMARY: Arachnoiditis ossificans is an uncommon end-stage appearance of chronic adhesive arachnoiditis. Imaging features of arachnoiditis ossificans are characteristic and should be diagnosed to avoid unnecessary intervention and guide prognosis and management. In this case series, we retrospectively analyzed CT and MR imaging of 41 patients to identify common patterns of intrathecal ossification and present the common etiologies. Thirty-two patients had a confirmed history of spinal instrumentation, 7 were discovered on imaging without prior surgical history, 1 had a history of ankylosing spondylitis, and 1 had trauma. The most frequent site of ossification was at the conus and cauda equina. Four patterns of ossification were identified, including central, nerve root encasing, weblike, and peripheral. Arachnoiditis ossificans is an important, likely under-recognized consideration in patients who present with back pain. Diagnosis can be made readily on CT; MR imaging diagnosis is also possible but may be challenging.

ABBREVIATION: AO = arachnoiditis ossificans

Chronic adhesive arachnoiditis is a spectrum of entities of varying severity and assorted imaging appearances. This pathologic entity involves the arachnoid mater layer of the meninges, which is often inconspicuous on cross-sectional imaging and becomes apparent in diseased states.[1] Chronic adhesive arachnoiditis predominates as thickening and scarring of the arachnoid and pial surfaces and can also involve the nerve roots. The typical features of chronic adhesive arachnoiditis include nerve root thickening, nerve root clumping, nerve root peripheralization (empty thecal sac), intradural soft-tissue masses, and thecal sac deformity, all of which can be visualized on MR imaging.[2,3] Chronic adhesive arachnoiditis is not associated with a specific etiology but rather can be seen following surgery, infection, inflammation, and/or trauma.[2,4] Some case reports have even demonstrated findings after intrathecal administration of medications such as contrast or chemotherapy.[5,6]

Arachnoiditis ossificans (AO) is an infrequent pathologic entity that appears on the spectrum of chronic adhesive arachnoiditis, often as the end-stage disease process.[2,7] In 1982, Barthelemy[8] published the first case of AO diagnosed on CT. Before this, AO was often suspected radiologically; however, it was only diagnosed surgically or at postmortem examination. Since that time, CT of the spine has allowed greater diagnosis of AO, with the largest case series documenting 5 patients.[3] The underlying histopathology in AO is thought to be osseous metaplasia in the setting of chronic arachnoid inflammation leading to intrathecal ossification.[9,10] However, despite chronic adhesive arachnoiditis being easily seen on MR imaging, arachnoid ossification can be inconspicuous and may, therefore, be overlooked or misdiagnosed. Although AO is a rare entity, it is likely more widespread than previously thought. CT is considered a more accurate imaging technique for AO because it can more accurately distinguish intrathecal AO from the overarching diagnosis of chronic adhesive arachnoiditis.[3,11]

The aim of this work was to identify patterns of ossification on CT that are characteristic of AO and can assist radiologists in making the correct diagnosis.

CASE SERIES

Institutional ethics review board at the Hospital for Special Surgery and Weill Cornell University-New York Presbyterian Hospital approval was obtained for this retrospective case series from an orthopedic surgical hospital as well as a tertiary trauma center for imaging studies performed between January 1, 2000, and July 1, 2021. Cases were acquired through a search of an institutional PACS, identifying patients with the diagnosis of AO on either CT or MR imaging with histopathologic confirmation.

Received October 27, 2022; accepted after revision December 19.

From the Department of Radiology and Diagnostic Imaging (B.T.), University of Alberta, Edmonton, Alberta, Canada; Department of Radiology and Imaging (C.S.G., J.L.C., S.T.J.), Hospital for Special Surgery, New York, New York; Department of Radiology (M.R), New York-Presbyterian Hospital, Weill Cornell Medicine, New York, New York; and Department of Pathology and Laboratory Medicine (D.J.P.), Weill Cornell Medicine, New York, New York.

Please address correspondence to Shari T. Jawetz, MD, Department of Radiology and Imaging, Hospital for Special Surgery, 535E 70th St, New York, New York; e-mail: jawetzs@hss.edu

http://dx.doi.org/10.3174/ajnr.A7764

Table 1: CT protocol used in spine imaging of the 41 patients included in the case series

CT Protocol	
kV(peak)	120
mAs	AutomA and SmartmAs with maximum dose 400 mA
Section thickness	0.625-mm section thickness, Bone Plus Algorithm
Reformations	Multiplanar reformations, 2-mm reformats in sagittal and coronal planes and to disc levels and in soft-tissue windows

Table 2: MR imaging protocol used in spine imaging of the 41 patients included in the case series

	2D Sagittal T2	2D Coronal T2	2D Axial T2	2D Sagittal T1	2D Sagittal T2 FLEX
TR (ms)	3500	4000	3500	620	5500
TE (ms)	110	104	110	10	110
Flip angle	180°	90°	180°	90°	142°
FOV (mm^2)	260	280	280	280	260
Matrix	512 × 256	512 × 256	416 × 224	512 × 256	416 × 224
NEX	1.5	1	1.5	1	1
Receiver bandwidth (MHz)	±83.33	±195.31	±83.33	±195.31	±244.14
Section thickness (mm)	3.5	3.5	3.5	3.5	3.5
Echo-train length	14	12	12	3	16
Acquisition time (min)	3–4	3–4	4–5	3–4	3–4

Note:– FLEX indicates 2-point Dixon fat-suppression.

Table 3: Demographics and characteristics of 41 patients with confirmed diagnosis of AO

Demographics and Characteristics	
Total patients	41
Age (yr)	63 (SD, 18.8); range, 16–92
Etiology	
Postsurgical	32
Idiopathic	7
Inflammatory	1
Posttraumatic	1
Sex	
Male	18
Female	23
Location	
Lumbar spine	36
Thoracic spine	5
Follow-up duration	3.9 (SD 3.7) years; range, 8 months to 14 years
No follow-up	18 patients
Patients with MR imaging correlation	25

The search yielded the following unique cases: 50 of AO, 383 of chronic arachnoiditis, 7 of intrathecal ossification, and 3 of intrathecal calcification. Cases without CT or pathologic confirmation were excluded. The electronic medical record was reviewed to collect data on patient demographics. Prior relevant surgical and medical history was acquired, including history of trauma, central nervous system infection, and inflammatory disease.

MR imaging was performed on a 1.5T unit (Optima MR450w, Discovery MR450, Signa HDxt; GE Healthcare) and on a 3T unit (Signa Premier; GE Healthcare). CT was performed using a 64-section scanner (Discovery 750 HD; GE Healthcare). Imaging protocols can be reviewed in Tables 1 and 2.

The patients' imaging studies were reviewed in consensus by 3 radiologists (a fellowship-trained musculoskeletal radiologist with 10 years' experience, a neuroradiologist with 2 years' experience, and a musculoskeletal radiology fellow). Imaging was evaluated for the presence of meningeal ossification, location of the ossification, associated spinal cord or nerve root distortion, and a pattern of ossification. Common patterns of ossification were described and categorized. When available, MR imaging was reviewed to evaluate corresponding lesions as well as associated signal abnormalities within the nerve roots and cord. The data sets were collected and collated in de-aggregate form. A series of 41 cases of AO was identified. A summary of patient demographics and characteristics is included in Table 3.

Four major etiologic categories were identified with the following frequency: 1 inflammatory, 1 posttraumatic, 7 idiopathic, and 32 postsurgical. A 38-year-old male patient with a remote history of gunshot wound to the thoracic and lumbar spine with follow-up imaging demonstrating lumbar spine AO (Fig 1) was included; this patient did not undergo any spinal surgery because he was hemiparetic at the time of injury. One patient with a history of ankylosing spondylitis was included, and, in addition to findings of AO, imaging demonstrated classic features of diffuse syndesmophyte ankylosis with a "bamboo spine" appearance, interspinous ligament ossification, and intradiscal calcification (Fig 2).

In 7 patients, AO was found without a history of symptoms, inciting events, or risk factors. One of these patients was a 24-year-old female gymnast presenting with low back pain without a history of known trauma, infection, or inflammatory disorder. Another case was a 20-year-old man who presented for whole-spine CT following a suicide attempt, and AO was discovered at the distal-most aspect of the thecal sac. AO was also found within the thoracic spine on a CT scan of the chest in 2 patients imaged for screening for lung nodules. In another patient, AO was found in the lumbar spine on a CT scan of the pelvis performed for evaluation of the hip joints. Pre-existing AO was found on 2 lumbar spine CT scans in 1 patient presenting for imaging in the setting of acute trauma and in another patient being evaluated for multiple myeloma.

The largest subset of patients consisted of 32 cases with a history of spinal surgery. Two patients underwent tethered cord release, 8 patients underwent laminectomy only, and 22 patients underwent combined laminectomy and instrumented arthrodesis (Fig 3). The diagnosis of AO was made in patients with a history of

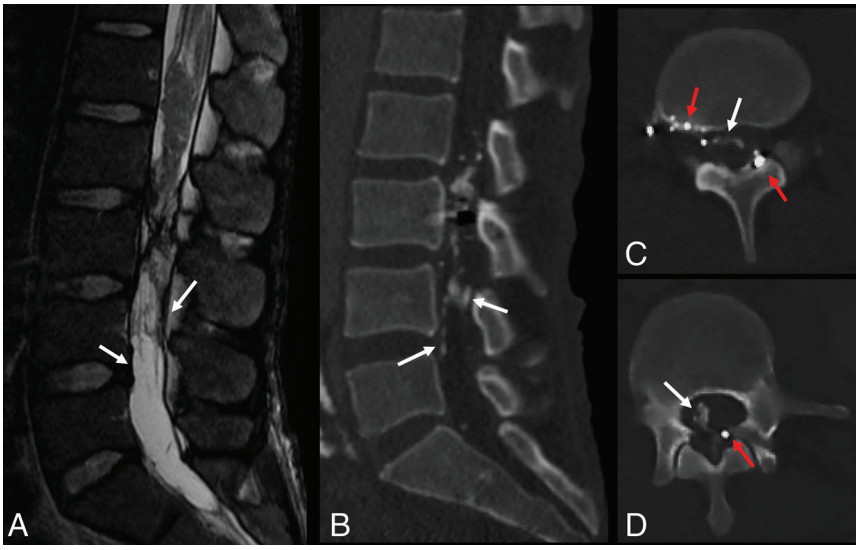

FIG 1. A 38-year-old male patient presenting 7 years following gunshot injury to the lumbar spine. Imaging from the time of the injury was unavailable for review. Sagittal T2-weighted MR imaging (*A*) demonstrates low signal thickening of the thecal sac as well as contour deformity of the thecal sac and its contents. Intermediate-signal tissue is present at the conus medullaris, relating to a posttraumatic scar. CT image (*B*) demonstrates peripheral and weblike ossification within the thecal sac (*white arrows*), which is not definitively identified on MR imaging (*white arrows*). The weblike ossification is better demonstrated on axial CT images (*C* and *D*), which also show multiple foci of metallic debris related to the prior gunshot injury (*red arrows*).

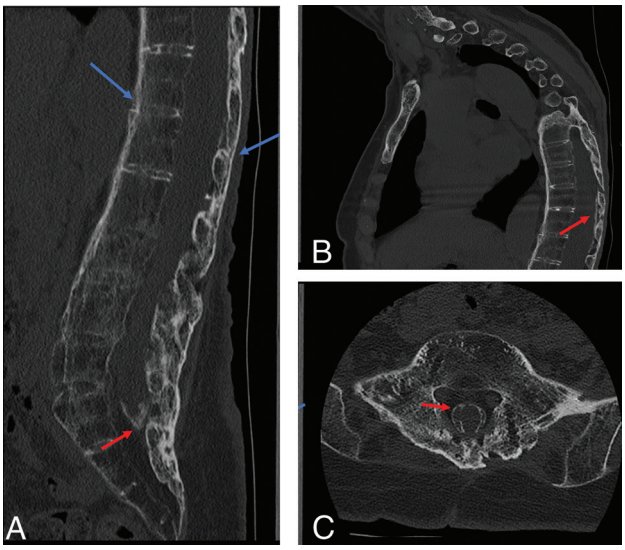

FIG 2. CT images from a 66-year-old female patient with back pain and stiffness. Sagittal (*A* and *B*) and axial (C) CT demonstrate features of spinal ankylosis relating to inflammatory spondyloathropathy (*blue arrows*). AO is evident by thick peripheral ossification of the meninges most prominent at the tip of the thecal sac; however, it can also be seen in the thoracic spine (*red arrows*).

surgery, on average, 13.4 (SD 14.7) years following the operation, with a range of 1–47 years. Of these patients, 1 underwent spinal fusion in the setting of a gunshot injury. All patients presenting following surgery had back pain. In 5 patients with history of spinal fusion, consecutive CT demonstrated progression of ossification in the setting of worsening of the patient's symptoms (Fig 4).

One patient with a history of tethered cord release developed lumbar spine AO and subsequently underwent surgical resection of the ossification. Histopathologic analysis was performed following staining with H&E. The resection specimen demonstrated peripheral areas of osseous formation along the margins of resected tissue, consisting of meningothelial cells within leptomeninges with scattered foci of calcification (Fig 5).

Review of all imaging demonstrated 4 typical patterns of ossification seen in our case series (Fig 6). Patients either presented with a dominant pattern or demonstrated a mixed presentation. The first observed pattern was peripheral ossification along the border of the thecal sac, which can be completely or partially circumferential; this pattern was observed in 8 patients. The second observed pattern was central longitudinal ossification within the thecal sac with a filamentous morphology on sagittal imaging, which was seen in 5 patients; depending on the location and appearance, this may represent ossification surrounding the filum terminale. The third pattern was weblike ossification that fills the CSF space and insinuates throughout the thecal sac; 7 patients presented with this pattern. Finally, a pattern in which the ossification encased ≥1 nerve root was seen in 3 patients. In 18 patients, a mixed pattern of ossification was observed, which predominated as a combination of central and peripheral as well as peripheral and weblike. In these patients, the 2 patterns contributed equally to the overall appearance of AO (Fig 7). In the 4 patients presenting with neurologic symptoms of unilateral lower extremity weakness, numbness, and neurogenic claudication, peripheral and nerve-encasing patterns of ossification were seen.

Twenty-five patients had both MR imaging and CT of the spine. MR imaging of the spine included sagittal and axial T1 and T2, coronal T2, and sagittal STIR sequences; gradient-echo sequences were not used and are not part of our routine nonsupervised MR imaging of the thoracic and lumbar spine. Regions of ossification demonstrated on CT corresponded to findings on MR imaging predominating as areas of low-signal-intensity thickening of the thecal sac and surrounding the nerve roots as well as clumping up the nerve roots and contour distortion of the thecal sac and nerve roots. Ossification was not reliably demonstrated on MR imaging. The findings demonstrated on MR imaging are not specific to AO and can be seen in the spectrum of chronic adhesive arachnoiditis. Of 25 patients, 23 had a history of spinal surgery, 1 had a gunshot injury, and 1 was in the incidental group. In all except 1 patient, MR imaging was performed before the CT scan. The only person who had a CT scan before MR imaging had sustained a gunshot wound to the thoracic spine. In the patients with a history of spinal instrumentation, all

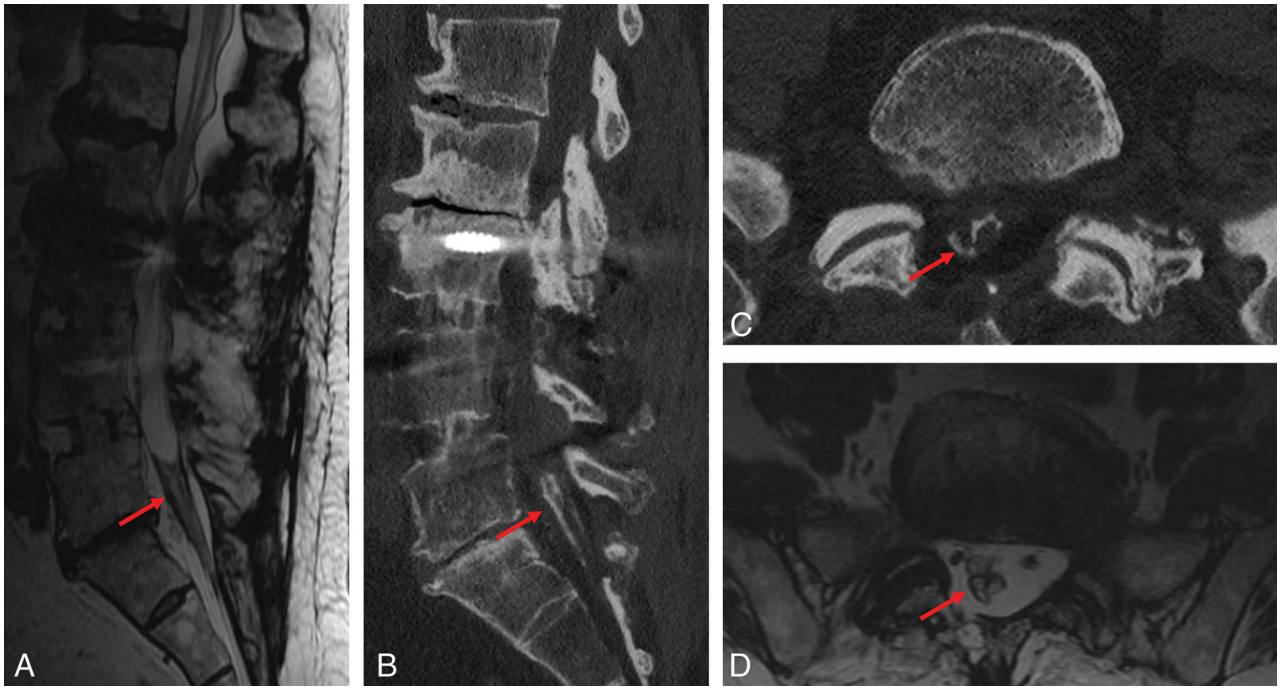

FIG 3. A 78-year-old man status post multiple lumbar surgeries. T2-weighted MR imaging of the lumbar spine including sagittal (*A*) and axial (*D*) reformats demonstrates low signal thickening of the thecal sac and surrounding the nerve roots (*red arrows*), which manifests as weblike ossification on sagittal (*B*) and axial (*C*) CT images (*red arrows*). MR images (*A* and *D*) depict the associated thecal sac distortion.

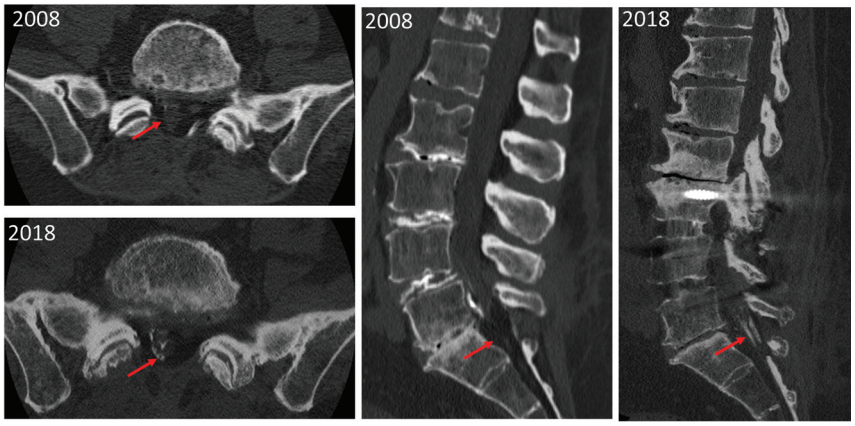

FIG 4. Comparison of CT scans of the lumbar spine of the same patient performed in 2008 with follow-up in 2018 demonstrates progression of ossification (*red arrows*), which potentially contributes to progression of pain and neurologic dysfunction.

underwent MR imaging followed by CT. CT was acquired to better evaluate fusion hardware and the cause of back pain.

DISCUSSION

Chronic adhesive arachnoiditis is a pathologic entity seen in the spine that includes a spectrum of severity. The most severe type, AO, is rare, and recognition is important in patients presenting with back pain and neurologic deficits.[2,12]

This is the largest published series of patients diagnosed with AO secondary to various etiologies. Within the published literature, case reports and series of AO confirmed on imaging can be found dating back to 1982.[8] Most of the published literature is limited to single case reports, with the largest case series including 5 patients.[3] The most common etiology for AO in the literature was spinal instrumented arthrodesis. Other etiologies included trauma, infection, spondyloarthropathy, intrathecal drug administration, and remote intrathecal contrast administration. The lumbar spine was the most common location for AO within the published case reports, with the second most common location reported in the thoracic spine;[6-9,13-21] no cases of cervical spine AO were reported. The most common clinical presentations were lower extremity weakness and back pain. Given this distribution, we believe that there is a link between location and etiology.

This series of patients was largely consistent with the demographics and characteristics of patients in the literature. In this series, 78% of patients had undergone spinal surgery, most whom underwent spinal decompression or fusion, which speaks to the prevalence of AO in this patient population. Thus, recognition is important given the increasing volume of spinal surgery.[22,23] While there are proposed treatment options primarily designed to restore CSF flow dynamics, such as attempts to lyse adhesions, these attempts have demonstrated limited success; therefore, AO should be considered a "do-not touch lesion"[3,24] because intervention does not lead to symptom improvement or prevent progression of the pathologic process. Like many pathologic processes without robust treatment, we believe that correct diagnosis of AO

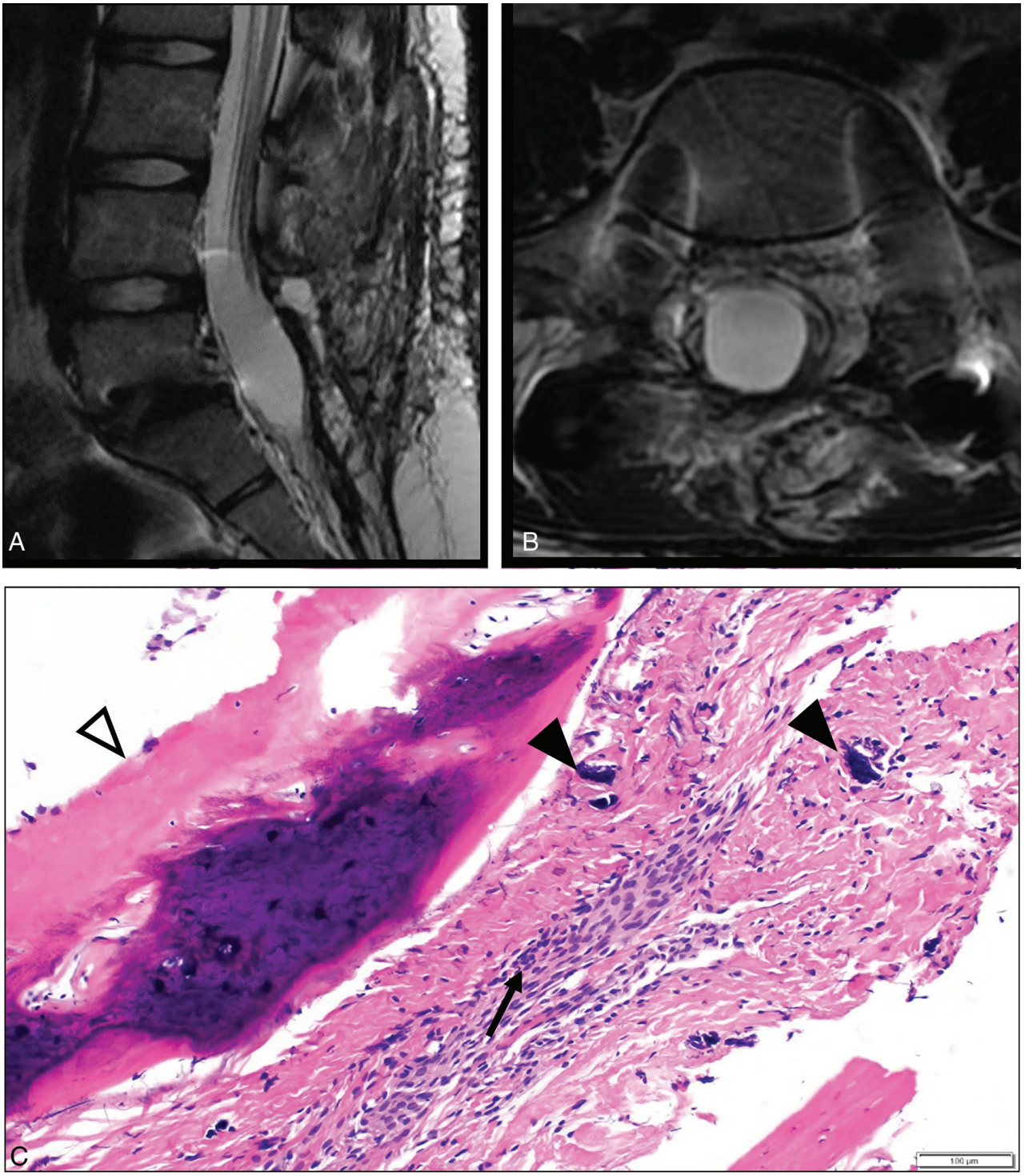

FIG 5. A 16-year-old female patient with a history of remote tethered cord release and posterolateral fusion. MR imaging T2-weighted images in the sagittal (*A*) and axial (*B*) planes demonstrate low signal thickening of the thecal sac with peripheralization and clumping of the nerve roots. *C*, H&E stains of the resection specimen from the thecal sac at the lumbar spine demonstrate meningothelial cells within the resected leptomeninges (*black arrow*), with ossification along the margin of the specimen (*white arrowhead*) as well as scattered foci of calcification (*black arrowheads*), consistent with AO.

is important, even in the absence of definitive treatment, because it may prevent unnecessary testing such as CSF sampling, biopsy, and even surgery, thus stressing the importance of acknowledging the various imaging appearances and patterns of AO to prevent misdiagnosis.

Most interesting, this series had 7 cases of idiopathic AO in patients who were reportedly asymptomatic. Given the retrospective nature of this study, clinical information in this group of patients was limited; thus, data were not always available to confirm the presence or absence of symptoms. This finding can be

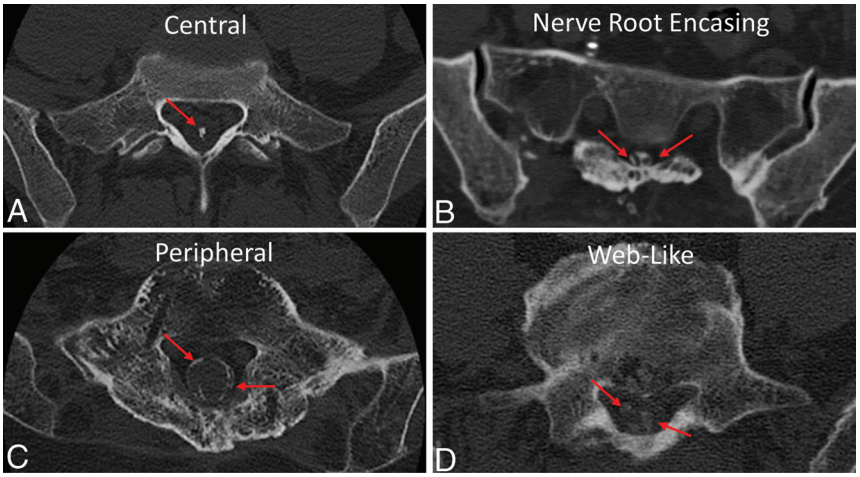

FIG 6. In this series of 41 patients, 4 patterns of ossification that can be seen in AO were identified. Ossification can occur as a combination of patterns, which was the most common in this series. CT images demonstrate the 4 patterns. *A*, The central pattern demonstrates central ossification within the thecal sac and can have the appearance of a dagger on the sagittal plane. *B*, Nerve root encasement appears as circumferential ossification surrounding single or multiple roots of the cauda equina. *C*, The peripheral pattern involves the walls of the thecal sac and can be circumferential or discontinuous. *D*, The weblike pattern appears as ossification filling the thecal sac and insinuating between the nerve roots. In all panels the *red arrows* point out the areas of ossification.

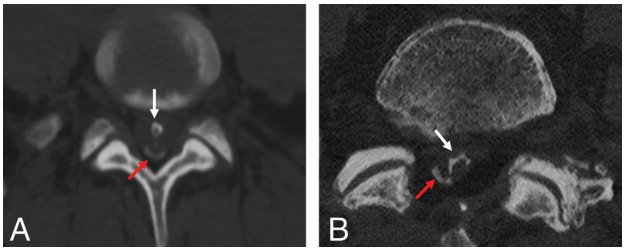

FIG 7. In some patients, a combined pattern of ossification was observed. Axial CT images in 2 unique patients demonstrate 2 patterns coexisting. *A*, The *red arrow* demonstrates the peripheral pattern of ossification coupled with a central pattern as shown by the *white arrow*. *B*. In this patient, the *red arrow* also indicates a region of peripheral ossification, coupled with weblike ossification as indicated by the *white arrow*.

interpreted in 2 major ways: One hypothesis is that not all patients experience symptoms from these ossifications; alternatively, the ossification may simply represent a "red herring" in the work-up of patients who have a multitude of reasons for back pain including failed back surgery. These findings further support the importance of recognizing AO as a do not touch lesion. Future prospective and longitudinal studies will be required to answer this question.

The patterns of ossification seen in AO can be variable as demonstrated in our series and within the literature. This variability may result in interpreters under-recognizing AO or mistaking it for another entity. In the literature, attempts have been made to characterize and classify the patterns of ossification. In a study by Domenicucci et al,[25] the authors proposed a classification system based on their review of 3 of their own case reports; however, the analysis is limited due to the small sample size. The large size of this series lends itself well to pattern analysis, and the most common ossification patterns were classified. The 4 main patterns of ossification identified, including peripheral, central, weblike, and nerve encasing, can serve as a guide for the physician interpreting CT of the spine when faced with meningeal ossification. Given the retrospective nature of this case series, it is difficult to associate the different patterns with the severity of symptoms or the presence of neurologic deficits. Most of these patients presented with symptoms of pain, with only 10% presenting with neurologic deficits including weakness and paresthesia. In patients with neurologic deficits, peripheral and nerve-encasing patterns of ossification were seen. This observation suggests that these patterns of ossification may correlate with patient symptoms. However, larger prospective studies are needed to determine this effect.

In 25 patients, MR imaging was available for review. However, the diagnosis of AO was not possible prospectively from the MR imaging nor were there specific MR imaging features to suggest AO. Theoretically, given the underlying osseous metaplasia driving AO, a centrally T1-hyperintense and peripherally hypointense lesion may be considered to represent AO; however, in our experience, the MR imaging finding predominates as T1/T2 low signal indicative of cortical bone. Allowing for the small size of the ossific lesion, the lower spatial resolution and higher section thickness of MR imaging can conceal the T1-hyperintense fatty medullary component of AO, which can be readily seen on CT as hypodensity. In these cases, MR imaging demonstrated low signal thickening of the thecal sac and nerve roots as well as nerve root clumping and contour distortion of thecal sac, all of which are nonspecific for AO and can be seen in the spectrum of chronic adhesive arachnoiditis.

CT remains the technique of choice for the diagnosis of AO. However, in many patients with back pain and neurologic symptoms, MR imaging may be indicated for diagnosis; thus, in these patients who undergo only MR imaging, AO may be underdiagnosed. Radiologists supervising these examinations may elect to add sequences such as fat-suppressed 3D-FLASH sequences[26] or a T2-weighted gradient recalled-echo sequence[27] for better imaging of cortical bone. These sequences have been reliably used for many years to image osseous morphology and are readily available at most imaging suites. Emerging techniques in MR imaging may, in the future, allow better identification of AO. One such technique is zero-TE, which allows better characterization of ossification and bone structures by acquiring signal immediately after applying the radiofrequency pulse, resulting in near-zero TEs, which allow imaging of structures with very short transverse relaxation times (T2) such as bones.[28] This technique is not currently widely used clinically and remains in the research phase; however, many studies evaluating musculoskeletal structures, specifically the spine,[29,30] have shown promise.

CONCLUSIONS

AO is an important consideration, likely underdiagnosed, in patients who present with back pain following spine surgery. CT is considered diagnostic for AO, and MR imaging is less reliable for definitive diagnosis though it is complementary in evaluating chronic adhesive arachnoiditis. Ossification can progress with time, and it is important to consider with worsening pain/weakness postoperatively. We present the largest series of patients with AO during a 20-year period and demonstrate patterns of ossification: peripheral, central, encasing nerve roots, and weblike.

Disclosure forms provided by the authors are available with the full text and PDF of this article at www.ajnr.org.

REFERENCES

1. Romano N, Castaldi A. **What's around the spinal cord? Imaging features of extramedullary diseases.** *Clin Imaging* 2020;60:109–22 CrossRef Medline
2. Peng H, Conermann T. **Arachnoiditis.** In: *StatPearls*. StatPearls 2021. http://www.ncbi.nlm.nih.gov/books/NBK555973/. Accessed January 10, 2022
3. Frizzell B, Kaplan P, Dussault R, et al. **Arachnoiditis ossificans: MR imaging features in five patients.** *AJR Am J Roentgenol* 2001;177:461–64 CrossRef Medline
4. Wright MH, Denney LC. **A comprehensive review of spinal arachnoiditis.** *Orthop Nurs* 2003;22:215–19; quiz 220–21 CrossRef Medline
5. Ward M, Mammis A, Barry MT, et al. **Novel association between intrathecal drug administration and arachnoiditis ossificans.** *World Neurosurg* 2018;115:400–06 CrossRef Medline
6. Wang S, Ahuja CS, Das S. **Arachnoiditis ossificans: a rare etiology of oil-based spinal myelography and review of the literature.** *World Neurosurg* 2019;126:189–93 CrossRef Medline
7. Whittle IR, Segelov JN. **Spinal arachnoiditis ossificans.** *Neurosurgery* 1983;13:737 CrossRef Medline
8. Barthelemy CR. **Arachnoiditis ossificans.** *J Comput Assist Tomogr* 1982;6:809–11 CrossRef Medline
9. Wijdicks CA, Williams JM. **Spinal arachnoid calcifications.** *Clin Anat* 2007;20:521–23 CrossRef Medline
10. Singh H, Meyer SA, Jannapureddy MR, et al. **Arachnoiditis ossificans.** *World Neurosurg* 2011;76:478.e12–14 CrossRef Medline
11. Bakhsh WR, Mesfin A, Bridwell KH. **Arachnoiditis ossificans after revision adolescent idiopathic scoliosis surgery: a 22-year follow-up and review.** *Spine (Phila Pa 1976)* 2013;38:E1166–70 CrossRef Medline
12. Anderson TL, Morris JM, Wald JT, et al. **Imaging appearance of advanced chronic adhesive arachnoiditis: a retrospective review.** *AJR Am J Roentgenol* 2017;209:648–55 CrossRef Medline
13. Abrams J, Li G, Mindea SA, et al. **Arachnoid ossificans containing metaplastic hematopoietic marrow resulting in diffuse thoracic intrathecal cysts and severe myelopathy.** *Eur Spine J* 2012;21(Suppl 4): S436–40 CrossRef Medline
14. Bagley JH, Owens TR, Grunch BH, et al. **Arachnoiditis ossificans of the thoracic spine.** *J Clin Neurosci* 2014;21:386–89 CrossRef Medline
15. Bailey D, Mau C, Rizk E, et al. **Arachnoiditis ossificans in the thoracic spine with associated cyst and syringomyelia: a rare, intraoperative finding complicating dural opening.** *Cureus* 2021;13: e16910 CrossRef Medline
16. Cosan TE, Kabukcuoğlu S, Arslantas A, et al. **Spinal toxoplasmic arachnoiditis associated with osteoid formation: a rare presentation of toxoplasmosis.** *Spine (Phila Pa 1976)*2001;26:1726–28 CrossRef Medline
17. Kahler RJ, Knuckey NW, Davis S. **Arachnoiditis ossificans and syringomyelia: a unique case report.** *J Clin Neurosci* 2000;7:66–68 CrossRef Medline
18. Papavlasopoulos F, Stranjalis G, Kouyialis AT, et al. **Arachnoiditis ossificans with progressive syringomyelia and spinal arachnoid cyst.** *J Clin Neurosci* 2007;14:572–76 CrossRef Medline
19. Slavin KV, Nixon RR, Nesbit GM, et al. **Extensive arachnoid ossification with associated syringomyelia presenting as thoracic myelopathy: case report and review of the literature.** *J Neurosurg* 1999;91:223–29 CrossRef Medline
20. Toribatake Y, Baba H, Maezawa Y, et al. **Symptomatic arachnoiditis ossificans of the thoracic spine: case report.** *Paraplegia* 1995;33:224–27 CrossRef Medline
21. Joković M, Grujicõić D, Bašcõarević V, et al. **Thoracal arachnoiditis ossificans associated with multifocal motor neuropathy: a case report.** *Br J Neurosurg* 2019 June 19 [Epub ahead of print] CrossRef Medline
22. Beschloss A, Ishmael T, Dicindio C, et al. **The expanding frontier of outpatient spine surgery.** *Int J Spine Surg* 2021;15:266–73 CrossRef Medline
23. Meara JG, Leather AJM, Hagander L, et al. **Global Surgery 2030: evidence and solutions for achieving health, welfare, and economic development.** *Lancet* 2015;386:569–24 CrossRef Medline
24. Scalia G, Certo F, Maione M, et al. **Spinal arachnoiditis ossificans: report of quadruple-triggered case.** *World Neurosurg* 2019;123:1–6 CrossRef Medline
25. Domenicucci M, Ramieri A, Passacantilli E, et al. **Spinal arachnoiditis ossificans: report of three cases.** *Neurosurgery* 2004;55:985 CrossRef Medline
26. Algin O, Gokalp G, Ocakoglu G. **Evaluation of bone cortex and cartilage of spondyloarthropathic sacroiliac joint: efficiency of different fat-saturated MRI sequences (T1-weighted, 3D-FLASH, and 3D-DESS).** *Acad Radiol* 2010;17:1292–98 CrossRef Medline
27. Tang MY, Chen TW, Zhang XM, et al. **GRE T2*-weighted MRI: principles and clinical applications.** *Biomed Res Int* 2014;2014:312142 CrossRef Medline
28. Weiger M, Brunner DO, Dietrich BE, et al. **ZTE imaging in humans.** *Magn Reson Med* 2013;70:328–32 CrossRef Medline
29. Argentieri EC, Koff MF, Breighner RE, et al. **Diagnostic accuracy of zero-echo time MRI for the evaluation of cervical neural foraminal stenosis.** *Spine (Phila Pa 1976)* 2018;43:928–33 CrossRef Medline
30. Hou B, Liu C, Li Y, et al. **Evaluation of the degenerative lumbar osseous morphology using zero echo time magnetic resonance imaging (ZTE-MRI).** *Eur Spine J* 2022;31:792–800 CrossRef Medline